Unconventional magnetic transitions in the mineral clinoatacamite $Cu_2Cl(OH)_3$

X. G. Zheng,[1,*] T. Kawae,[2] Y. Kashitani,[2] C. S. Li,[2] N. Tateiwa,[2] K. Takeda,[2] H. Yamada,[3] C. N. Xu,[3] and Y. Ren[4]
[1]*Department of Physics, Saga University, Saga 840-8502, Japan*
[2]*Faculty of Engineering, Kyushu University, Fukuoka 812-8581, Japan*
[3]*National Institute of Advanced Industrial Science and Technology, Tosu, Saga 841-0052, Japan*
[4]*Argonne National Laboratory, 9700 S. Cass Avenue, Argonne, Illinois 60439, USA*
(Received 20 July 2004; revised manuscript received 27 October 2004; published 24 February 2005)

Unconventional magnetic properties are found for a quantum spin system of mineral clinoatacamite, $Cu_2Cl(OH)_3$. Clinoatacamite is found to undergo an antiferromagnetic transition at 18.1 K with a small entropy fall ($0.05R \ln 2$). At temperatures below 6.4 K, it transits into a disordered spin-glass-like state but with large specific heat anomalies. The entire entropy fall for the spin system is about $0.31R \ln 2$, which is smaller than those for dipolar spin ice ($0.67R \ln 2$) and for ice I_h ($0.71R \ln 2$). Geometric frustration for the quantum Cu^{2+} spins is suggested based on its crystal structure, magnetization, and specific heat studies.

DOI: 10.1103/PhysRevB.71.052409 PACS number(s): 75.75.+a, 75.20.−g, 75.90.+w

Geometric frustration has become a central subject in condensed matter physics since the discovery of the "spin ice state" in pyrochlores of $Dy_2Ti_2O_7$ and $Ho_2Ti_2O_7$.[1] A macroscopic degeneracy of ground states and finite zero-point entropy has been suggested for both ice and spin ice.[1–3] New ordered state and physics about strong electron correlation are expected with studies on spin ice. Exploration of new materials that can be considered to be related to or compared with the spin ice is of great importance. The forces in pyrochlores that dominate the magnetic interactions between the spins are magnetic dipole-dipole interactions that arise from the large magnetic moments of the rare earth ions Ho^{3+} and Dy^{3+}. Here we report a quantum exchange spin system as a candidate for geometric frustration. Experimental evidence on magnetization and specific heat suggests that clinoatacamite is an interesting quantum spin system for the study of geometric frustration and a possible reference system for the study of spin ice.

Recently we observed features of disorder and geometric frustration in the minerals of $Cu_2Cl(OH)_3$. $Cu_2Cl(OH)_3$ has three polymorphs: atacamite[4] in orthorhombic structure ($a=6.030$ Å, $b=6.865$ Å, $c=9.120$ Å), botallackite[5] in monoclinic structure ($a=5.717$ Å, $b=6.126$ Å, $c=5.636$ Å, $\beta=93.07°$), and clinoatacamite[6] in monoclinic structure ($a=6.157$ Å, $b=6.814$ Å, $c=9.104$ Å, $\beta=99.65°$). We succeeded in preparing pure-phase samples for the individual structures and have made it clear that they are three magnetic materials. Both atacamite and botallackite are antiferromagnets with Néel temperatures of $T_N=9.0$ K and $T_N=7.2$ K, respectively.[7,8] A muon spin rotation (μSR) study shows that a long-range order develops in botallackite with distinct muon spin rotation frequencies, while atacamite shows a broad distribution in the internal field created by the Cu^{2+} spins despite its single-crystal nature.[9] The crystal structure of botallackite is similar to that of $Cu_2C_mH_{2m+1}(OH)_3$, which is considered to be a two-dimensional (2D) triangular quantum Heisenberg antiferromagnetic lattice.[10,11] Atacamite can be considered as a distorted 3D lattice of corner-sharing tetrahedrons of Cu^{2+} spins, and this image can explain the randomness of the magnetic field in atacamite.[9] Most interesting results are observed for clinoatacamite. The feature of the 3D network of corner-sharing tetrahedrons of Cu^{2+} spins (Fig. 1, lower panel) is strikingly similar to that of pyrochlores. Therefore, more frustrated antiferromagnetism (AFM) than atacamite is expected for clinoatacamite. Detailed structure parameters for synthetic clinoatacamite are summarized in Table I. The position of Cl in the structure is much farther from the Cu^{2+} ions than the O ions; therefore, antiferromagnetic interac-

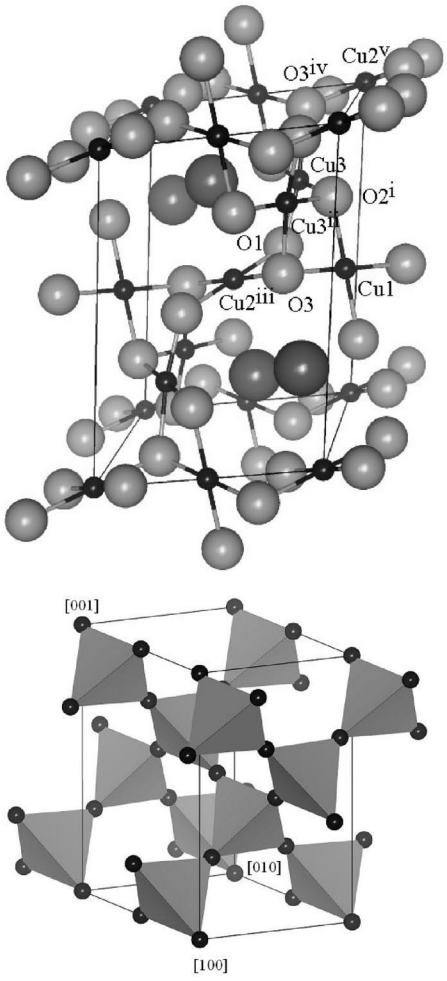

FIG. 1. Crystal structure of clinoatacamite showing the 3D network of corner-sharing tetrahedrons of Cu^{2+} ions (black balls).

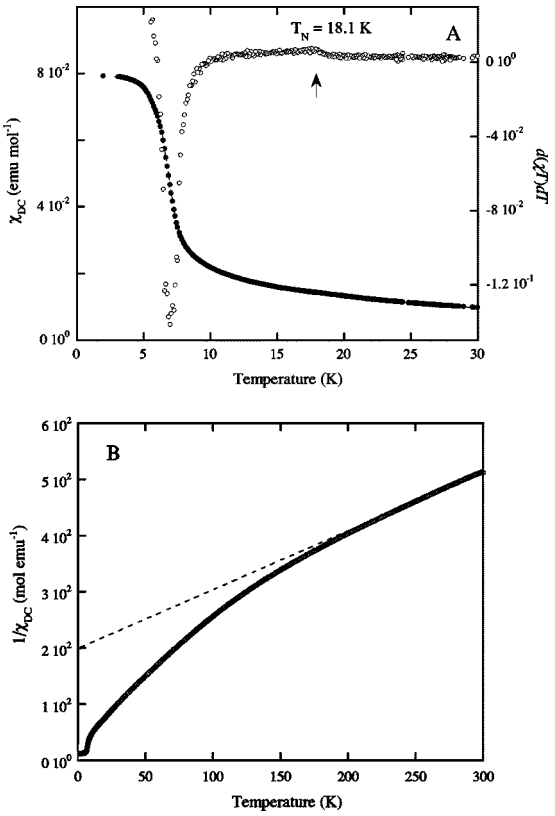

FIG. 2. (A) Temperature dependence of the dc susceptibility. The arrow helps to show a magnetic transition at 18.1 K. (B) temperature dependence of reciprocal dc susceptibility. The dashed line follows a Curie-Weiss law of $\chi \sim A/(T+190\ \mathrm{K})$.

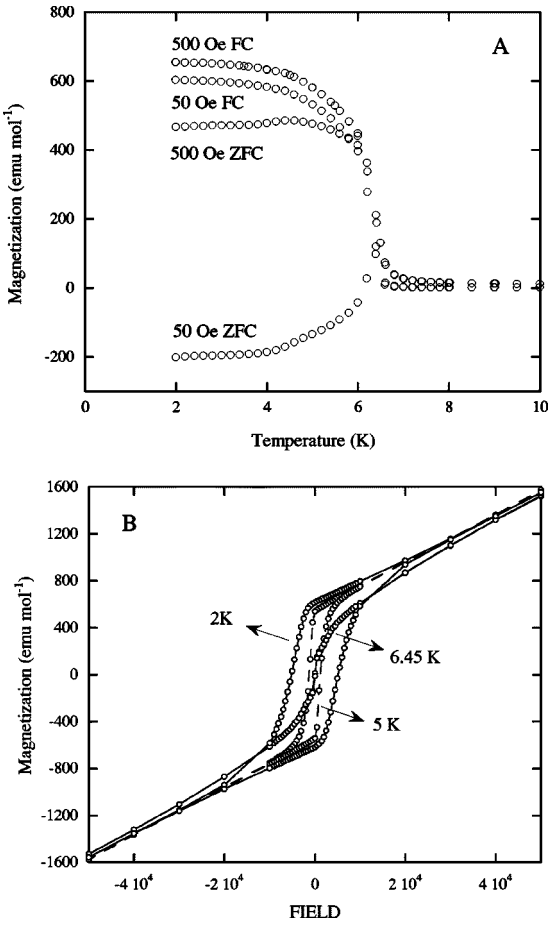

FIG. 3. (A) Temperature dependence of magnetization under zero-field cooling and field cooling conditions; (B) field dependence of magnetization.

tions should be through the Cu-O-Cu bonds.

Synthetic polycrystalline clinoatacamite was prepared using a solution reaction from 100 g of $Cu(HCOO)_2 \cdot 4H_2O$ and 40 g of KCl in purified water (at 95 °C). Polycrystalline clinoatacamite precipitates were thoroughly washed and filtered. The crystalline nature was further improved by a hydrothermal treatment at 200 °C. The pure phase of the reported clinoatacamite structure with $a=6.1637(2)$ Å, $b=6.8166(3)$ Å, $c=9.1140(3)$ Å, and $\beta=99.6515(15)°$ was confirmed by synchrotron powder x-ray diffraction at beam line BL02B2, SPring-8 (detailed structure parameters are listed in Table I). Investigation with transmission electron microscopy further confirmed that there was no secondary phase impurity. dc as well as ac magnetic susceptibility measurements were performed with an assembly of ca. 30 mg of clinoatacamite particles using a commercial SQUID magnetometer (Quantum Design; MPMS-7S). ac susceptibility measurements were carried out at various frequencies and dc fields (the amplitude of the ac field was fixed to 1 Oe). Heat capacity was measured by an adiabatic heat pulse method with a ^{3}He cryostat using an amount of 0.7547 g of the clinoatacamite particles.

The temperature dependence of the dc susceptibility (at 10 kOe) is shown in Fig. 2(a). A rapid increase in susceptibility was observed below 7 K. Subsequently, a decrease in the slope was recognized near 6 K. For short-range order or frustrated antiferromagnetic systems where the magnetic transition can hardly be recognized on the susceptibility-temperature plot, the differential plot of $d(\chi T)/dT$ is often used to distinguish the transition temperature.[12] This technique finds a transition near 18.1 K, as shown in Fig. 2(a). As described later, this transition is verified by the specific heat measurement. In addition, a preliminary μSR experiment clearly showed that this is the antiferromagnetic Néel temperature. Measurement of the dc susceptibility up to 300 K showed that the Curie-Weiss law predicts a much higher value, with T_N of ca. 190 K (Fig. 2(b)), suggesting that the antiferromagnetism is frustrated. The magnetization measured under the zero-field cooling (ZFC, in the remnant field of the superconducting magnet, which is approximately 6 Oe) and field cooling (FC) conditions showed an anomaly peak around 6.2 K (Fig. 3(a)) similar to those of a spin glass, suggesting that the system is demagnetized in zero field at low temperatures. At 2 K, a remnant magnetization of 0.05 μ_B/Cu is produced after applying a dc field (Fig. 3(b)). These behaviors might be found in a conventional spin-glass system. However, the following ac susceptibility and heat capacity measurements show that it is not a usual spin glass.

Figure 4(a) shows the temperature-dependence curves of the ac susceptibility (the real part χ' and imaginary part χ'') at various frequencies. The steep rise below 7 K and anomalies at temperatures denoted by $T_{f1}=6.4$ K and $T_{f2}=6.2$ K were observed. Together with the behaviors with increasing

TABLE I. Structure information of synthetic clinoatacamite.

Compound name	Clinoatacamite
Chemical formula	$Cu_2Cl(OH)_3$
Cell setting	Monoclinic
Space group	$P2_1/n$ (no. 14)
Z	4
a (Å)	6.1637(2)
b (Å)	6.8166(3)
c (Å)	9.1140(3)
β (deg)	99.6515(15)
V (Å^3)	377.51(2)
D (g cm^{-3})	3.70
R_{wp} (S)[a]	0.0732 (5.06)
R_B	0.0487

Atom	Site	g	x	y	z	U (10^{-2} Å^2)
Cu1	2e	1	0	1/2	1/2	0.72(4)
Cu2	2d	1	0	0	0	0.72
Cu3		1	0.2590(6)	0.2358(4)	0.7468(5)	0.72
Cl	2e	1	0.1130(4)	−0.0044(10)	0.3080(4)	1.41(9)
O1	2e	1	0.311(2)	0.2883(16)	0.5513(13)	1.26(14)
O2	4f	1	0.4255(13)	−0.008(2)	0.7789(9)	1.26
O3	2e	1	0.2523(19)	0.6844(16)	0.5362(13)	1.26

Bond length (Å)		Bond angle (deg)	
Cu1—O3	1.984(11)	Cu1—O2—Cu3^{ii}	98.985
Cu1—O2^{i}	1.991(8)	Cu1—O3—Cu3^{ii}	96.781
Cu2^{iii}—O1	1.960(13)	Cu1—O2^{i}—Cu3	99.486
Cu2^{iii}—O3	2.047(12)	Cu1—O3—Cu2^{iii}	99.731
Cu3—O1	1.896(13)	Cu2^{iii}—O1—Cu3	124.334
Cu3^{ii}—O2^{i}	1.947(13)	Cu3—O3^{iv}—Cu2^{v}	114.402
Cu3—O3^{iv}	2.021(12)		
Cu3—O2^{i}	2.078(13)		

Symmetry codes: i, $^{-}x^{+}1/2$, $y^{+}1/2$, $^{-}z^{+}3/2$; ii, $^{-}x^{+}1/2$, $y^{+}1/2$, $^{-}z^{+}3/2$; iii, $^{-}x^{+}1/2$, $y^{+}1/2$, $^{-}z^{+}1/2$; iv, $^{-}x^{+}1/2$, $y^{-}1/2$, $^{-}z^{+}3/2$; v, x, y, $z^{+}1$.

[a] $S=R_{wp}/R_e$

the frequency of the ac field, they suggest that after the sample transits into a weak ferromagnetic state, the magnetic moments are quickly frozen below T_{f1}, then further frozen at T_{f2}. The freezing temperatures move to higher temperatures in a superimposed dc field (Fig. 4(b)). The insensitivity to frequency and the enhancement of the anomaly temperatures in the dc field distinguish it from a usual spin glass.

The specific heat clearly shows a phase transition near 18.1 K (Fig. 5(a)) that corresponds to $T_N=18.1$ K in Fig. 2(a). A larger peak appears below 7 K with shoulders at 6.4 K and 6.2 K, respectively, which is consistent with low-temperature anomalies in the ac susceptibilities (Fig. 5(b)). The change of the shape under magnetic field suggests that they are magnetic transitions. Besides, no change in the lattice between 2 and 20 K was observed with a low-temperature synchrotron x-ray diffraction study. Estimation of the entropy shows a very small entropy fall ($0.05R\ln 2$) for the antiferromagnetic transition at 18.1 K, suggesting that the spins are only partially ordered in the antiferromagnetic state. An antiparallel "up-down" spin arrangement cannot be satisfied for the Cu^{2+} spins in the tetrahedron, however, like the triangular lattice in botallackite, a chiral structure with four apical spins pointing to the center of the tetrahedron can ensure a Néel ground state.

There might be other explanations for the experimental results observed, such as canted antiferromagnetic structure. However, we have observed basically the same behaviors (large coercivity, small moment, glassiness, and clear phase transition) with $\sim\mu$m particles (the results presented here) as well as with fine powders of poorer crystallinity ($\sim$10 nm−0.1 μm). The only difference is that with the improved crystallinity, the phase transition at 18.1 K and the anomalies at 6.4 K and 6.2 K become clearly evident. The small entropy at 18.1 K transition suggests a partial freezing of the spin freedom. These experimental results cannot be consistently explained by the canted antiferromagnetism.

The most surprising aspect is that the total entropy fall is around $0.31R\ln 2$, that is, ca. 1/3 of the total spin entropy.

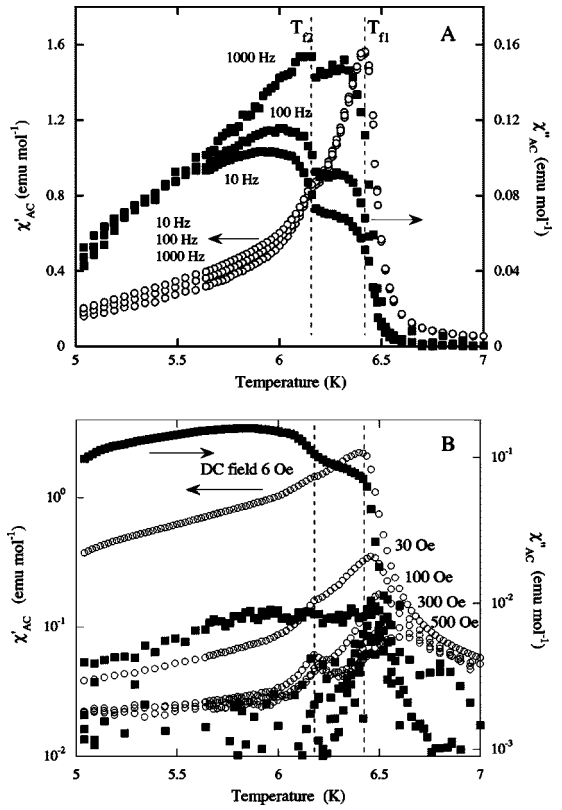

FIG. 4. (A) Real and imaginary parts of ac magnetic susceptibilities χ' and χ'' measured at varied frequencies (10, 100, and 1000 Hz, respectively); (B) ac susceptibilities (plotted on a logarithm scale) in dc fields at 1 Hz. Dashed lines denote freezing temperatures.

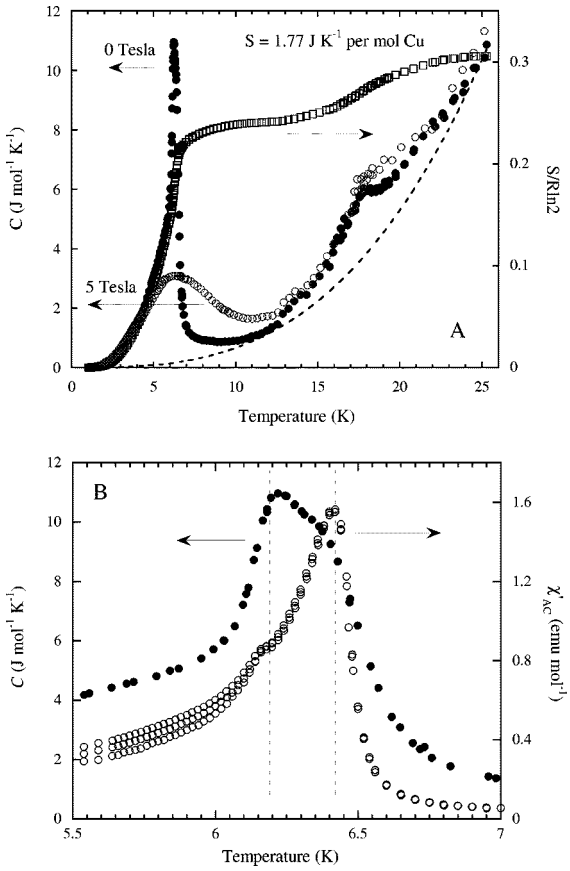

FIG. 5. (A) Temperature dependence of the specific heat (per mol of the molecule) at zero field and 5 T, respectively, and the magnetic entropy; the dashed line represents the lattice contribution according to Debye's law. (B) An enlarged view of the zero-field specific heat in the low temperature range showing consistency to the anomalies in the ac susceptibility.

It is unlikely that additional entropy is developed below 1 K because the specific heat drops by more than three orders of magnitude from 6 to 1 K indicating near-complete spin freezing. The finite zero-point entropy is around $(1-0.31)R\ln 2$, which is even larger than $(1-0.67)R\ln 2$ in the dipolar spin ice and that of $(1-0.71)R\ln 2$ in ice. Despite the difference in the spin interactions such that the pyrochlore has a ferromagnetic dipolar interaction between the rare earth ions while clinoatacamite shows an antiferromagnetic quantum exchange interaction between Cu^{2+} spins, both show incomplete order due to geometric frustration and infinite entropy like the ice. This consistency strongly suggests that the clinoatacamite is a geometric frustrated spin system that may be compared with the pyrochlores.

In summary, the geometric structure of corner-sharing tetrahedrons of the magnetically coupled Cu^{2+} spins, the freezing of magnetic moments, and the incomplete entropy fall all suggest the possibility that clinoatacamite can be viewed as new type of geometric frustration for quantum Heisenberg spins. We expect neutron diffraction and theoretical studies on clinoatacamite, especially because the magnetic dynamics in this *d*-electron system, should be easier to theoretically model than the *f* electrons in the pyrochlore. The revealed properties of the structure-correlated properties of *d* electrons in this natural cuprate might also contribute to the study of magnetic interactions in the superconducting cuprates.

This work is supported by a Grant-In-Aid for Scientific Research to X.G.Z. from the Japan Society for the Promotion of Science (JSPS).

*Author to whom correspondence should be addressed. Email address: zheng@cc.saga-u.ac.jp

[1] M. J. Harris *et al.*, Phys. Rev. Lett. **79**, 2554 (1997).
[2] Pauling, *The Nature of the Chemical Bond* (Cornell University Press, Ithaca, New York, 1945).
[3] A. P. Ramirez *et al.*, Nature (London) **399**, 333 (1999).
[4] J. B. Parise and B. G. Hyde, Acta Crystallogr., Sect. C: Cryst. Struct. Commun. **42**, 1277 (1986).
[5] F. C. Hawthorne, Miner. Mag. **49**, 87 (1985).
[6] J. Grice *et al.*, Can. Mineral. **34**, 73 (1996).
[7] X. G. Zheng *et al.*, Solid State Commun. **130**, 107 (2004).
[8] X. G. Zheng *et al.*, Solid State Commun. **131**, 509 (2004).
[9] X. G. Zheng *et al.* (unpublished).
[10] M. A. Girtu *et al.*, Phys. Rev. B **57**, R11 058 (1998).
[11] M. A. Girtu *et al.*, Phys. Rev. B **61**, 4117 (2000).
[12] E. E. Bragg and M. S. Seehra, Phys. Rev. B **7**, 4197 (1973).